

## HIGH RESOLUTION STUDIES OF SMALL PARTICLES OF GOLD AND SILVER

### I. Multiply-twinned particles

L.D. MARKS

*Cavendish Laboratory, University of Cambridge, Madingley Road, Cambridge, CB3 0HE, UK*

and

David J. SMITH

*High Resolution Electron Microscope, University of Cambridge, Free School Lane, Cambridge, CB2 3RQ, UK*

Received 20 February 1981

The structure of multiply-twinned particles of gold and silver found in the early stages of particulate growth has been studied using direct lattice imaging methods with the Cambridge University 600 kV high resolution electron microscope. There was widespread evidence for the presence of strain-relieving partial dislocations in icosahedral particles. However, the possibility of imaging artefacts arising from double diffraction due to overlapping tetrahedral projections needed to be excluded, for example by slight particle tilting, before the actual presence of the dislocations was substantiated. An analysis of particle geometry, also including the effects of inhomogeneous strain, showed that straight Moiré fringes did not necessarily indicate the absence of strain within a particle. Moreover, it has been shown that, in some particle orientations, two different, though very similar, Moiré fringes can arise with their interaction and final appearance being very dependent on particle orientation.

### 1. Introduction

The most straightforward, and potentially the most powerful, method for examining small particles (ca. 10 nm or less) is direct lattice imaging in a high resolution electron microscope. In addition to observing any internal defects, an effective micro-diffraction pattern is obtained with very high spatial resolution. Three major problems arise: the image is not a complete representation of the object as the microscope does not faithfully transfer the contrast and position of all the lattice information; secondly, it is difficult to ensure that any strains are suitably projected so as to be visible and readily interpretable in the image; and finally, severe anomalies can occur through thickness variation and strains [1], particularly in the presence of dislocations [2].

It is well-known that small metal particles often exist in the form of decahedral and icosahedral mul-

tiple-twinned particles\* consisting of five and twenty tetrahedra respectively, as drawn schematically in fig. 1., with twinning on their (111) planes (for detailed discussion see refs. [3–6]). MTPs are normally found in the early stages of growth of small face-centered-cubic (fcc) particles, but can be grown to very large sizes (ca. 50  $\mu\text{m}$ ) by a variety of processes (see, for example, ref. [7]). It also appears that they may be of significance in catalysis [8]. It should be noted that tetrahedra with perfect fcc structure cannot be arranged to be completely space-filling. Previously, this has been taken to imply that some sort of lattice distortion (i.e. inhomogeneous strain or dislocations) must be present (e.g. ref. [5]). No observations of dislocations appear to have been reported [6], except

\* The abbreviations MTP for multiply-twinned particle, Dh for the decahedral form and Ic for the icosahedral form, will be used henceforth.

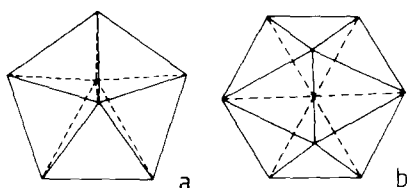


Fig. 1. Schematic models of the multiply-twinned particle: (a) decahedron; (b) icosahedron.

in large ( $\sim 100$  nm) MTPs [9,10]. Heinemann and colleagues [11–14] have, however, recently proposed new structural models for MTPs, based on a non-fcc structure, which do not require the presence of dislocations or non-uniform lattice strains.

Using the Cambridge University 600 kV high resolution electron microscope (HREM) [15,16], we have undertaken a detailed study of the internal and surface structure of small, vapour-deposited, metal particles [17]. Recent results have established, unambiguously, the presence of dislocations in Ics at least as small as 15 nm in diameter as well as indicating that the structure of more complicated “polyparticles” can be characterised directly [18]. This paper presents an account of our observations of both decahedral and icosahedral MTPs of silver and gold. Other particle types are considered in a subsequent paper [19].

## 2. Experimental details

Gold and silver were evaporated onto NaCl, and KCl, respectively, at  $300^\circ\text{C}$  in a vacuum of  $3 \times 10^{-3}$  Pa, the substrates having been previously cleaved in-situ. The samples were allowed to cool to room temperature in the vacuum (taking  $\sim 45$  min), and were then coated by evaporation with a thin amorphous carbon film, and mounted on microscope grids via flotation on distilled water. These samples were examined using axial illumination lattice imaging at accelerating voltages of 500 and 575 kV, principally the former, with the 600 kV HREM. An objective aperture was often used which included the (220) beams (0.144 nm), although its absence did not materially affect the images obtained. Typical operating conditions were with image magnifications of

300,000 to 400,000 times, considerably defocussed illumination (to ensure adequate illumination coherence), and exposure times of 4.5 or 7.5 s. Any residual image astigmatism was normally corrected at magnifications in excess of 600,000 times, using the granularity of the carbon support film.

## 3. Results

The general appearance of the samples is shown in figs. 2 and 3.

### 3.1. Decahedral MTPs

These particles are generally found with either  $\langle 100 \rangle$  or  $\langle 111 \rangle$  epitaxies, although some were also

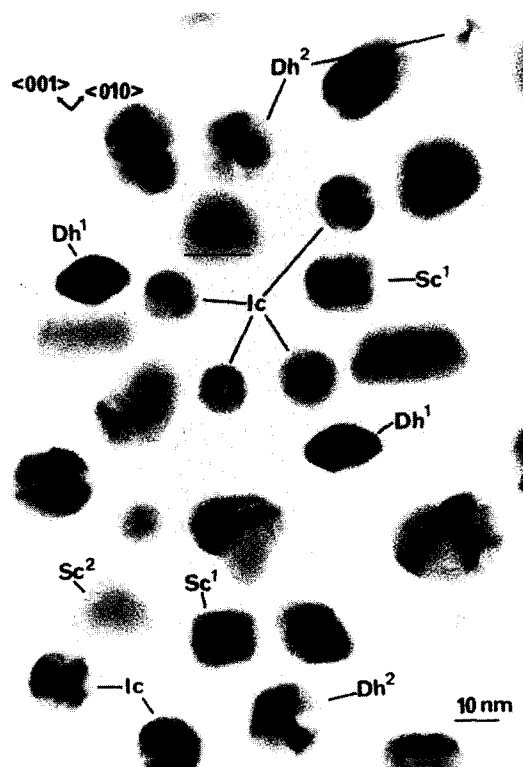


Fig. 2. A typical region of the silver sample. The different particle types indicated are: icosahedral MTPs (Ic); decahedral MTPs,  $\langle 100 \rangle$  and  $\langle 111 \rangle$  epitaxy (Dh<sup>1</sup>, and Dh<sup>2</sup> respectively); and single crystals with  $\langle 100 \rangle$  (Sc<sup>1</sup>) and  $\langle 111 \rangle$  (Sc<sup>2</sup>) epitaxy. The orientation of the substrate is also shown.

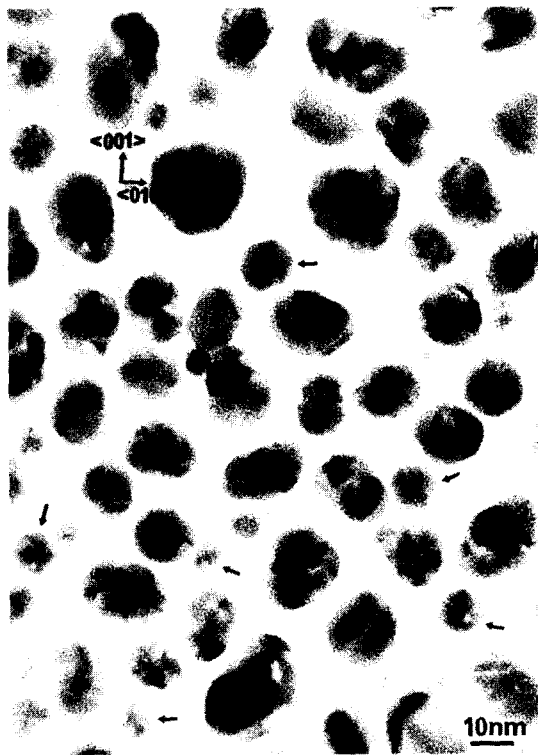


Fig. 3. A typical region of the gold sample. The principal particle types are icosahedral MTPs (arrowed) and more complicated polyparticles (see ref. [19]). The epitaxial directions of the substrate are indicated.

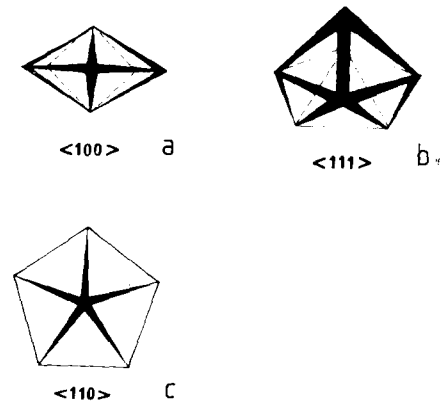


Fig. 4. Models showing the structure of the Dh projected in three principal directions: (a)  $\langle 100 \rangle$ ; (b)  $\langle 111 \rangle$ ; (c)  $\langle 110 \rangle$ .

who have previously shown that variations in thickness of a crystal can result in the position, and direction, of lattice fringes being altered.

The appearance of a typical  $\langle 111 \rangle$  epitaxed Dh is shown in fig. 6. At first sight, there appears to be little useful information to be obtained from a particle in this orientation. However, as we discuss in detail below, considerable care is required in the interpretation of the  $(111)/(220)$  Moiré fringes, as arrowed, or erroneous conclusions about the internal structure of the MTP and the presence, or otherwise, of inhomogenous strains may result.

observed in the  $\langle 110 \rangle$  orientation. A graphical representation of the Dh geometry in these three projections is given in fig. 4.

In the  $\langle 100 \rangle$  orientation an involved, but characteristic, lattice fringe pattern is observed, as shown in fig. 5. The very complicated appearance of these particles, especially in the central region, is due to simultaneous imaging of fringes of several different spacings: two (200) and one (111) primary lattice fringes of spacings 0.204 and 0.235 nm respectively, as well as two 0.286 nm, one 0.355 nm and one 0.695 nm Moiré fringes arising from double diffraction effects. Of particular interest is the distinct kink in the 0.286 nm Moiré fringes along the line marked AB which is due to a sharp change in the slope of the particle (i.e. reversal in sign of the thickness vector) at this point. This is not unexpected, given the work of Hashimoto et al. [1] in particular

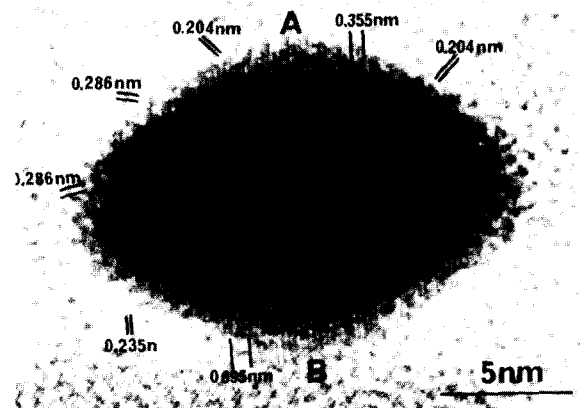


Fig. 5. Micrograph of a  $\langle 100 \rangle$  epitaxed Dh with various fringe spacings labelled. Note the kink in the 0.286 nm double diffraction fringes across the line AB due to the reversal in sign of the thickness vector, as indicated.

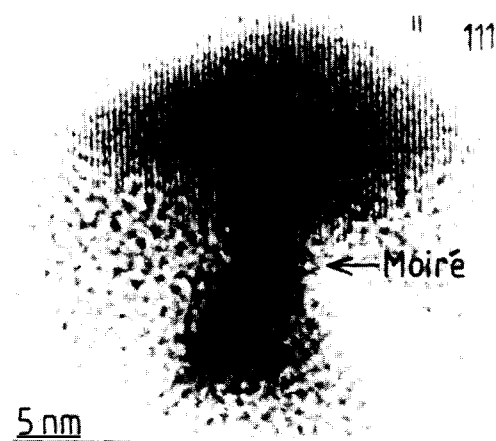


Fig. 6. Micrograph of a  $\langle 111 \rangle$  epitaxied Dh. The  $\langle 111 \rangle$  lattice fringes are slightly bent either as a result of inhomogeneous strain or due to small changes in the thickness vector.

Sometimes the particles are found tilted to a further orientation, namely the  $\langle 110 \rangle$  (see fig. 7). In such Dh's, some apparent defects are often visible which might be tentatively identified as partial dislocations. If these are of edge type, then they are indeed in the correct positions for a  $7.5^\circ$  (i.e. com-

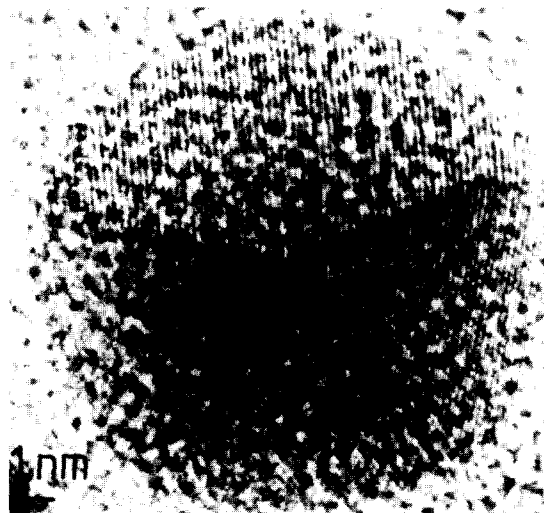


Fig. 7. Micrograph of a Dh close to the  $\langle 110 \rangle$  orientation. Two possible partial dislocations are indicated but note that these may be artefacts originating from thickness fringe phase shifts.

pletely strain relieving) grain boundary. However, it should be noted that there is an alternative, more likely explanation. Careful examination reveals the presence of thickness fringes with  $\xi_g^{\text{eff}} \sim 8.5$  nm. The half fringe phase shifts, with which these are known to be associated [1], are just visible in the particles and are the probable cause of these effects.

### 3.2. Icosahedral MTPs

The icosahedral MTP has no  $\langle 100 \rangle$  surfaces, in contrast to the decahedral form, and so has no  $\langle 100 \rangle$  epitaxy. For silver, in fact, a complete  $\langle 112 \rangle$  epitaxy (i.e. along a twin boundary) is observed with the  $\langle 111 \rangle$  and  $\langle 110 \rangle$  planes in two of the microcrystallites parallel to the substrate  $\langle 100 \rangle$  planes. For gold, the epitaxy is either  $\langle 111 \rangle$  or, to a lesser extent,  $\langle 112 \rangle$ , similar to that reported by Heinemann et al. [11]. A graphical representation of the Ic in these two projections is provided in fig. 8.

The lattice fringe structure seen in the typical  $\langle 112 \rangle$  oriented particle is shown in fig. 9. The large Moiré fringes present in these particles had rather complicated forms, with the exact configurations varying from particle to particle. Occasionally these fringes display a "split" appearance (see fig. 10a), similar to that observed by Gillet et al. [20]. As we will show in our analysis of the particle geometry below, this behaviour is not necessarily indicative of the presence of any form of grain boundary as suggested by Gillet et al. Fig. 10b shows the particle imaged in fig. 10a after it has been tilted by  $0.4^\circ$ . Note that the appearance of these Moiré fringes has altered considerably.

A large number of apparent partial dislocations were observed in these particles as, for example, indicated in fig. 9. In many cases, it is possible to confirm these as being real lattice defects, rather than

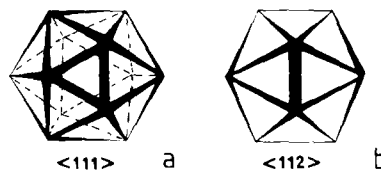


Fig. 8. Models showing the structure of the Ic projected in two directions: (a)  $\langle 111 \rangle$ ; (b)  $\langle 112 \rangle$ .

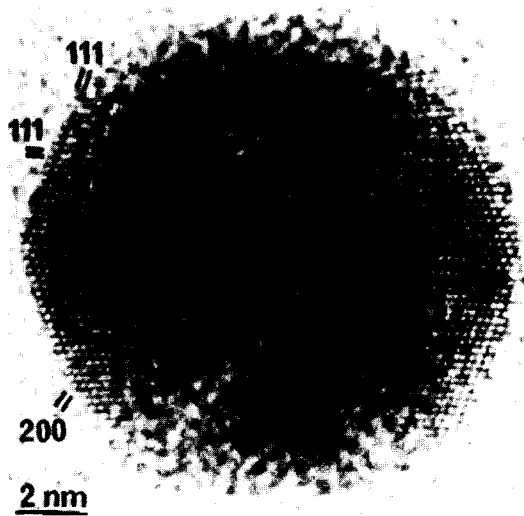


Fig. 9. Micrograph of a  $\langle 112 \rangle$  oriented Ic with two possible partial dislocations arrowed. Note the slightly bent lattice fringes and the complicated appearance of the (222) – (220) Moiré fringes.

artefacts of the imaging process, by tilting the specimen. As well as can be judged using the lattice imaging technique, the location of these defects within the various Ics remains constant, which would not

be the case should their appearance arise solely from double diffraction. A typical Ic with a defect satisfying this criterion is shown in fig. 11. It is also interesting to note that there appears to be very little diffraction contrast associated with these dislocations. This is presumably because the strains required to close the Ics are largely cancelling the normal dislocation strain field. This may be the reason why dislocations have not previously been identified in small MTPs.

One final feature of interest in these particles is the appearance of the (111) fringes along the edges of some of the segments. These are slightly bent, following the general shape of the particle. From a single micrograph it is clearly impossible to ascertain whether thickness variations or local strains are the cause. However, it was observed that the general structure of these fringes remained the same upon tilting by small amounts, suggesting that the bend in the fringes is due to some form of inhomogeneous strain. Image simulations are in progress to verify this possible explanation.

Typical examples of the  $\langle 111 \rangle$  epitaxed Ics are shown in fig. 12. The (111)/(220) Moiré fringes present in these particles were again relatively straight. In common with the similar situation occurring for the Dh, this establishes very little about the presence or

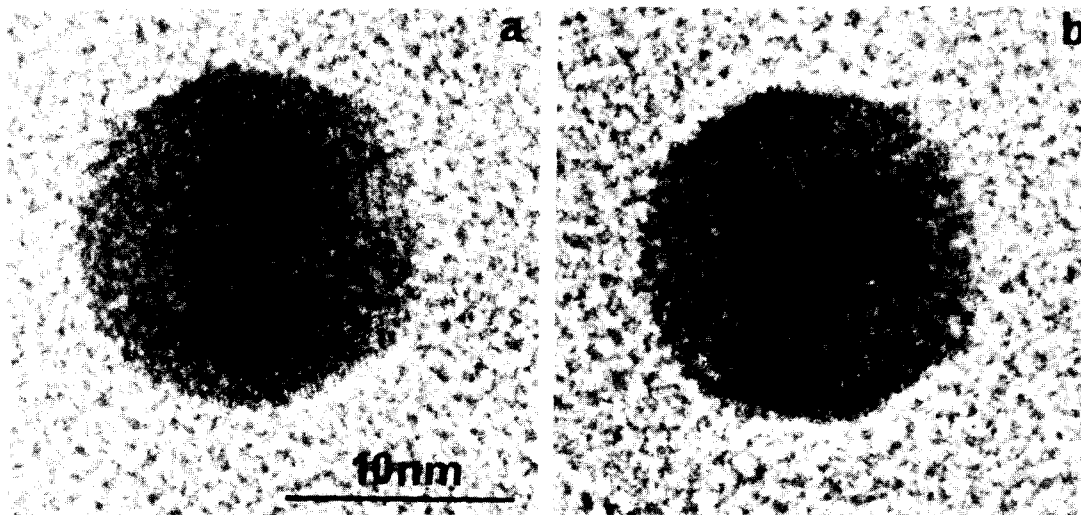


Fig. 10. (a) Ic close to the  $\langle 112 \rangle$  orientation, (b) same particle after tilting by  $0.4^\circ$ . Note the considerable change in appearance of the large Moiré fringes.

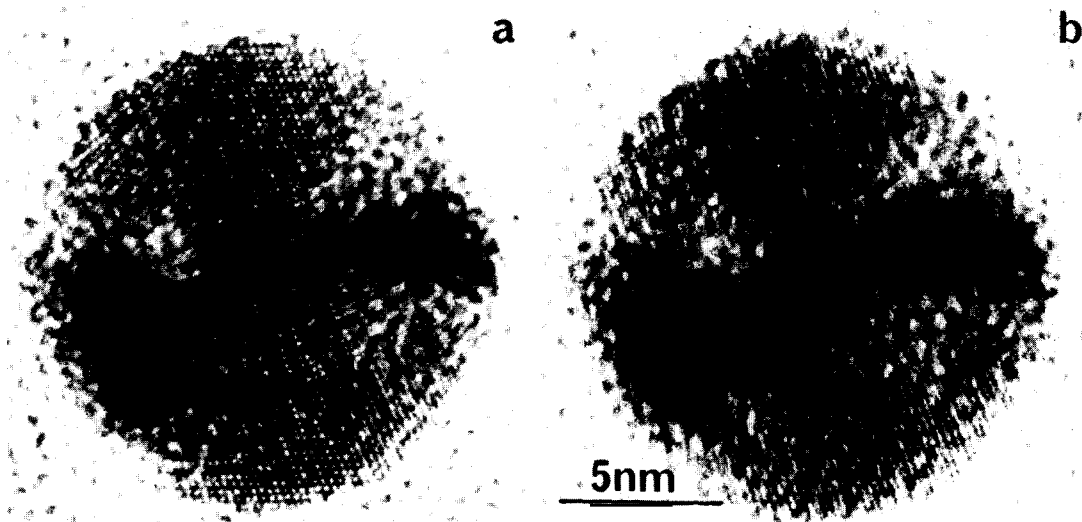


Fig. 11. (a) Typical Ic in the  $\langle 112 \rangle$  orientation, (b) same particle after tilting by  $0.5^\circ$ . Note that the relative position and appearance of the partial dislocation arrowed does not change with tilting.

absence of inhomogeneous strains. Note that dislocations, again tentatively identified as edge partials, were clearly imaged in most of the Ics in this orientation.

### 3.2.1. Analysis of Moiré fringes

A major source of confusion in the analysis of

small metal particles lies in the interpretation of small variations in any double diffraction Moiré fringes which originate from overlapping microcrystallite projections. The object of this section is to clarify somewhat the precise origin of these fringes, and the type of effects that might be expected when a rotational displacement field is present in an MTP, in

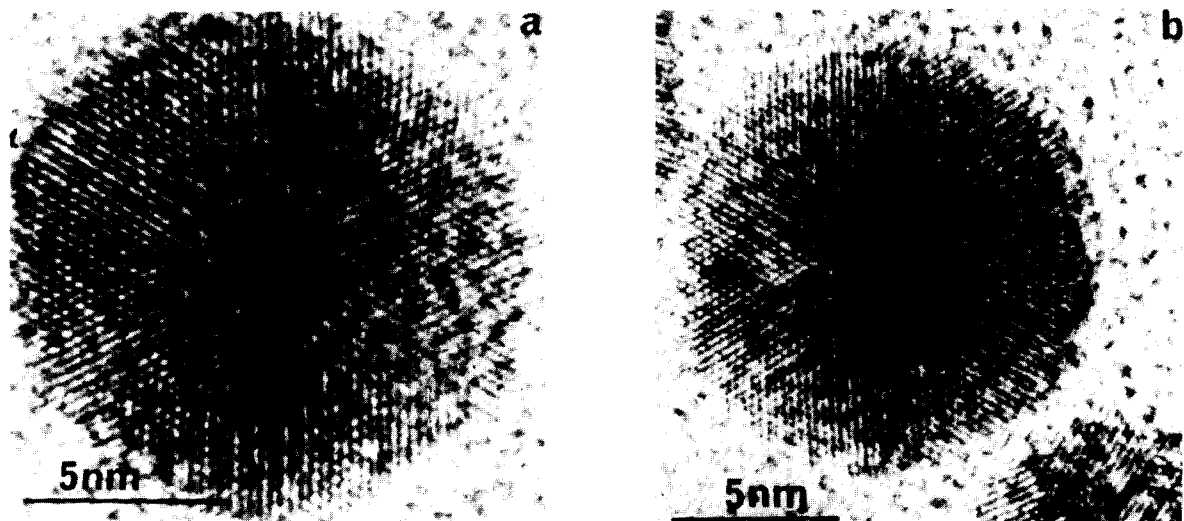


Fig. 12. Ics in the  $\langle 111 \rangle$  orientation with possible partial dislocations indicated: (a) silver; (b) gold.

order that possible erroneous interpretations based on their appearance might be avoided.

Consider first the (222) – (220) Moiré fringes in a  $\langle 111 \rangle$  oriented Dh which arise when two tetrahedral sections (labelled ABCD and ABCE in fig. 13a) overlap another tetrahedron (ABFG). It might be anticipated that if a rotational strain field is assumed, then the normal, rotated Moiré fringe approach could be employed. However, this is in fact incorrect. Although a rotational displacement rotates radial lines, the effects upon a set of parallel lines (i.e. the atomic planes) are far smaller, and less straightforward. Indeed, as noted by de Wit [21], the actual displacements, when using inhomogeneous isotropic elasticity theory with a plane strain, almost vanish when drafted accurately. The effects upon Moiré fringes could be correspondingly small. Fig. 13b shows a computer simulation of their appearance, drafted using de Wit's solution [21], superimposing the appropriate segments. It is clear that the observed rotations are vanishingly small. Hence, the occurrence of straight Moiré fringes should not be cited as evidence against the presence of inhomogeneous strains, as done previously by Heinemann et al. [11]. Note that very similar situations arise in both the  $\langle 111 \rangle$  and  $\langle 112 \rangle$  oriented Ics: similar qualifications on image interpretation must be applied.

In the particular case of the  $\langle 112 \rangle$  oriented Ic it does not appear to be appreciated that two different overlapping Moiré fringes can be obtained with almost identical orientation and spacing. As explained

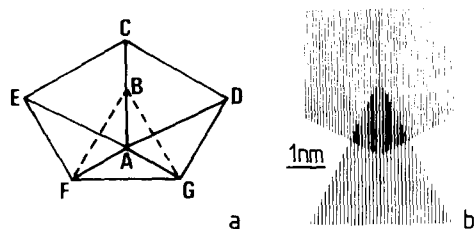


Fig. 13. (a) Representation of a  $\langle 111 \rangle$  oriented Dh. The tetrahedron ABGF is nominally  $\langle 111 \rangle$  oriented, with the other relevant tetrahedra, namely ABCE and ABCD, approximately  $\langle 112 \rangle$  oriented. (b) Computer simulation of the (222) – (220) Moiré fringes in a  $\langle 111 \rangle$  oriented Dh, showing the result of superimposing the (222) and (220) lattice planes after applying a rotational strain to each tetrahedron separately.

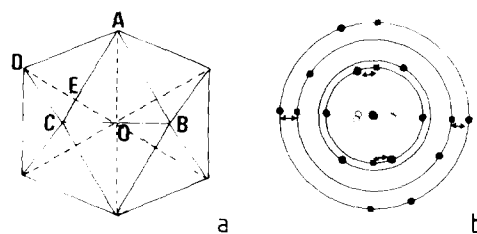


Fig. 14. Representation of (a) a  $\langle 112 \rangle$  oriented Ic and (b) diffraction from the tetrahedra ABOC (squares) and ADOA<sup>1</sup> (filled circles) (A<sup>1</sup> is beneath A). Double diffraction, as indicated on (b) by the arrows, produces two large spacing Moirés, shown by the empty circles, in region OAE.

in fig. 14, double diffraction between two (111) fringes can occur, leading to a spacing of  $\sim 0.695$  nm, as well as the (222) – (220) Moiré of  $\sim 0.69$  nm which is rotated by about  $9^\circ$  with respect to the former. With the fringe spacings and orientations so similar, it is to be expected that these will effectively combine to produce only one set of Moirés in the final micrograph, with the resultant depending on the relative strengths of each component: Small variations in particle orientation, which might occur during transfer onto the carbon support film, or when the specimen is tilted, will then lead to considerable variations in appearance, as already shown in fig. 10.

#### 4. Discussion

It is readily apparent from the images above that direct lattice imaging represents a particularly powerful method for examining small metal particles and providing valuable information about their internal structure. However, as we have emphasised, because of the likelihood of image artefacts occurring, micrographs recorded at different particle orientations are necessary pre-requisites before any firm conclusions about the presence and nature of lattice defects and strains can be made unambiguously.

It is unclear at this stage whether dislocations will always occur in the range of particle sizes observed: it is possible that the method of preparation is of importance. Certainly it does not appear that the dislocations are being induced by radiation dam-

age. For example, the electron beam might nucleate dislocations near the surface which could glide in. These would, however, leave behind stacking faults running to the surface, but these were not apparent. Note that observation of the dislocations using weak-beam dark-field methods might be anticipated to be rather difficult since those observed here appear to be nearly parallel to two of the symmetry orientations and also because, as commented earlier, the extent of the dislocation strain field is restricted by the internal strain of the particle. Conversely, the presence of so many dislocations in these Ics does not seem too surprising since, without any such lattice defects, the internal strains would be very large: a solid angle deficit of  $\sim 12\%$  has to be made up. The frequent absence of any stacking faults suggests that these occur as growth defects rather than via surface nucleation, although particle coalescence could sometimes be of importance, providing sufficient disturbance for their formation. Further studies of MTPs of different sizes, prepared under different conditions, are in progress to clarify these possibilities.

#### Acknowledgements

The Cambridge University 600 kV high resolution electron microscope has been built as a joint project between the Cavendish Laboratory and the Department of Engineering with major financial support from the Science Research Council, from which continued support is gratefully acknowledged. We thank Dr. A. Howie for many useful discussions.

#### References

- [1] H. Hashimoto, M. Mannami and T. Naiki, *Phil. Trans. Roy. Soc.* 253 (1961) 459, 490.
- [2] D.J.H. Cockayne, J.R. Parsons and C.W. Hoelke, *Phil. Mag.* 24 (1971) 139.
- [3] S. Ino, *J. Phys. Soc. Japan* 21 (1966) 346.
- [4] S. Ino and S. Ogawa, *J. Phys. Soc. Japan* 22 (1967) 1365.
- [5] J.G. Allpress and J.V. Sanders, *Surface Sci.* 7 (1967) 1.
- [6] T. Komoda, *Japan. J. Appl. Phys.* 7 (1968) 27.
- [7] M. Gillet, *Surface Sci.* 67 (1977) 139.
- [8] C. Disgurd, M.G. Maurin and J. Roberts, *Met. Corres. Ind.* 51 (1976) 255, 320.
- [9] L.D. Marks and A. Howie, *Nature* 282 (1979) 196.
- [10] Y. Saito, S. Yatsuya, K. Mihama and R. Uyeda, *Japan. J. Appl. Phys.* 17 (1978) 1 49.
- [11] K. Heinemann, M.J. Yacaman, C.Y. Yang and H. Poppa, *J. Crystal Growth* 47 (1979) 177.
- [12] M.J. Yacaman, K. Heinemann, C.Y. Yang and H. Poppa, *J. Crystal Growth* 47 (1979) 187.
- [13] C.Y. Yang, *J. Crystal Growth* 47 (1979) 274.
- [14] C.Y. Yang, M.J. Yacaman and K. Heinemann, *J. Crystal Growth* 47 (1979) 283.
- [15] W.C. Nixon, H. Ahmed, C.J.D. Catto, J.R.A. Cleaver, K.C.A. Smith, A.E. Timbs, P.W. Turner and P.M. Ross, in: *Developments in Electron Microscopy and Analysis 1977*, Ed. D.L. Misell (Institute of Physics, Bristol, 1977) p. 13.
- [16] V.E. Cosslett, *Proc. Roy. Soc. (London)* A370 (1980) 1.
- [17] L.D. Marks, A. Howie and D.J. Smith, in: *Electron Microscopy and Analysis 1979*, Ed. T. Mulvey (Institute of Physics, Bristol, 1980) p. 397.
- [18] D.J. Smith and L.D. Marks, *Phil. Mag.*, in press.
- [19] D.J. Smith and L.D. Marks, *J. Crystal Growth* 55 (1981) ...
- [20] E. Gillet, A. Renou and M. Gillet, *Thin Solid Films* 29 (1975) 2, 217.
- [21] R. de Wit, *J. Phys. C5* (1972) 529.